



The Compact Muon Solenoid Experiment
Conference Report

Mailing address: CMS CERN, CH-1211 GENEVA 23, Switzerland



15 September 2015 (v4, 23 September 2015)

CMS results on heavy flavour and quarkonia

Yongsun Kim for the CMS Collaboration

Abstract

The CMS collaboration has recorded 150 inverse microbarns and 35 inverse nanobarns of PbPb and pPb collisions, at 2.76 TeV and 5.02 TeV, respectively. This presentation reports the results of the heavy quark measurements including quarkonia and B mesons. A particular emphasis is given to the most recent results regarding the suppression of J/ψ , $\Psi(2S)$ and the Υ states in Pb+Pb collisions, and the study of cold nuclear matter effects based on p+Pb collisions.

Presented at *SQM2015 Strangeness in Quark Matter*

CMS Heavy Ion Results on Heavy Flavour and Quarkonia

Yongsun Kim on behalf of the CMS collaboration

Korea University, 145 Anam-ro, Seonbuk-gu, Seoul, Republic of Korea

E-mail: kimy@cern.ch

Abstract. The CMS collaboration has recorded $150 \mu\text{b}^{-1}$ and 35nb^{-1} of PbPb and pPb collisions at 2.76 TeV and 5.02 TeV respectively. This presentation reports the results of the heavy quark measurements including quarkonia and B mesons. A particular emphasis is given to the most recent results regarding the suppression of J/ψ , $\psi(2S)$ and Υ 's in PbPb collisions, and the study of cold nuclear matter effects based on pPb collisions.

1. Introduction

Understanding the production mechanisms of quarkonium bound states, from first principle calculations based on quantum chromodynamics (QCD), remains an open question in proton-proton (pp) and heavy ion collisions. In pp collisions, despite the extensive progress, none of the existing models can reproduce simultaneously the cross sections and polarization results measured experimentally. In heavy ion collisions, it was predicted that the Debye screening of the heavy quark potential would result in a sequential suppression of the quarkonium states reflecting their binding energies [1]. The quarkonium production can be affected also by several other processes apart from the existence of QGP, such as the nuclear parton distribution functions (nPDFs), parton energy loss, and nuclear absorption [2]. For this reason, the study of quarkonium production in pA collisions, besides PbPb and pp, is critical in order to understand and disentangle such Cold Nuclear Matter (CNM) effects.

This conference proceeding reports the measurement of J/ψ , $\psi(2S)$, Υ in pp, pPb and PbPb data collected during Run I period of CMS experiment. In addition, B meson results in pPb collisions are also discussed to study the CNM effects on open heavy flavor hadrons.

2. Experimental setup and analysis

2.1. CMS detector

A detailed description of the CMS detector can be found in Ref. [3]. Its central feature is a superconducting solenoid with an internal diameter of 6 meter, providing a magnetic field of 3.8 T. Within the field volume are the silicon pixel and strip tracker, the crystal electromagnetic calorimeter, and the brass/scintillator hadronic calorimeter. The silicon pixel and strip tracker measure charged-particle trajectories in the range $|\eta| < 2.5$. It consists of 66 million pixel and 10 million strip sensor elements. Muons are detected in the range $|\eta| < 2.4$, with detection planes based on three technologies: drift tubes, cathode strip chambers, and resistive plate chambers. Because of the strong magnetic field and the fine granularity of the tracker, the muon

p_T measurement based on information from the tracker alone has a resolution between 1 and 2% for typical muons in this analysis.

The CMS apparatus also has extensive forward calorimetry, including two steel/quartz-fiber Čerenkov hadron forward calorimeters (HF), which cover $2.9 < |\eta| < 5.2$. These detectors are used for online event selection and the impact parameter-like characterization of the events such as centrality in PbPb.

2.2. Reconstruction of quarkonia and B mesons

Analyses in this report commonly use muons as the basic object and quarkonia are identified via their di-muon decay channels. To extract the quarkonia yields, unbinned maximum likelihood fits to the $\mu^+\mu^-$ invariant mass spectra are performed. In general, the Υ and J/ψ resonances are modelled by the sum of two Crystal Ball (CB) functions, that is, Gaussian resolution functions with the low side tail replaced with a power law describing final state radiation. Given the relatively large statistical uncertainties of the 2.76 TeV samples, most of the parameters are fixed to values provided by simulations, then allowed to vary to compute the associated systematic uncertainties. The background is modelled by an exponential function multiplied by an error function describing the low-mass turn-on.

J/ψ and $\psi(2S)$ peaks are fitted simultaneously using the same invariant mass distribution. At mid-rapidity, a CB function describes well the J/ψ signal. At forward rapidity, due to rapid changes in muon resolution with $|\eta^\mu|$, the addition of a Gaussian function, with same mean m_0 but different width than the CB function, is needed to obtain a good fit. Various other fits are also performed to compute the systematic uncertainty.

The B^+ meson is reconstructed by combining a J/ψ with an extra track, while B^0 , B_s^0 candidates are reconstructed by combining a J/ψ with two tracks. For four-prong channels ($B^0 \rightarrow J/\psi K^*(892)$ and $B_s^0 \rightarrow J/\psi \phi$), two selected tracks are required to originate from a common vertex to form a $K^*(892)$ or a ϕ candidate. Finally, the two muons together with the tracks are required to form a B-meson candidate with the constraint that the di-muon invariant mass is equal to the nominal mass value of J/ψ . B-meson candidates with rapidity in the center-of-mass frame $|y_{CM}| < 1.93$ and $p_T > 10\text{GeV}/c$ are stored for further analysis.

Measured yields are corrected for acceptance and efficiency obtained from Monte Carlo (MC) simulation and further corrected by a data-driven technique called tag-and-probe [4].

3. Analysis methods and Results

3.1. $\Upsilon(nS)$ in PbPb

The yields of $\Upsilon(1S)$, $\Upsilon(2S)$ and $\Upsilon(3S)$ mesons are reported, from PbPb and pp data sets at the same center-of-mass energy of $\sqrt{s_{NN}} = 2.76$ TeV, corresponding to $166 \mu\text{b}^{-1}$ and 5.4pb^{-1} , respectively [5]. With respect to the previous result [6], the PbPb data reconstruction was improved yielding an increase of $\approx 30\%$ in the $\Upsilon(1S)$ yields. The pp dataset, recorded in 2013, is new and allows for further differential studies as functions of the Υ rapidity (y) and transverse momentum. R_{AA} are derived from the PbPb and pp yields

Figure 1 shows R_{AA} as a function of centrality, displayed as the number of participating nucleons, N_{part} . The global, fully-correlated uncertainties come from the uncertainty in the pp cross sections (which is different for the two Υ states) and the PbPb tracking efficiency. The strong centrality dependence, already observed in Ref. [6], is mapped out with more precision. The dependence of R_{AA} on kinematic variables is found to be weak as shown in figure 2.

3.2. J/ψ and $\psi(2S)$ in PbPb

The cross-section results of J/ψ and $\psi(2S)$ are reported in the form of double ratio (Fig. 3), instead of R_{AA} so that efficiency and acceptance corrections cancel to a large extent, reducing the systematic uncertainties.

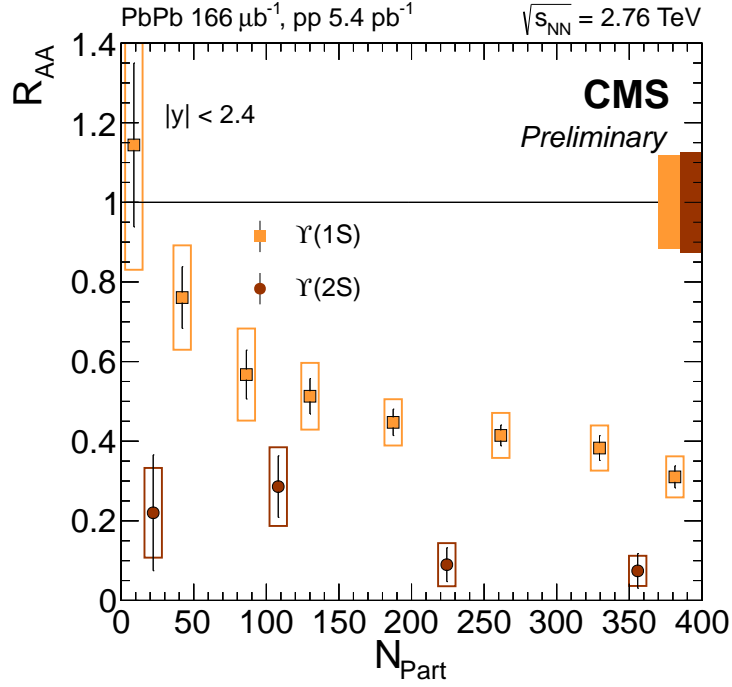


Figure 1. Nuclear modification factor of $\Upsilon(1S)$ and $\Upsilon(2S)$ in PbPb as a function of centrality, displayed as the number of participating nucleons. Statistical (systematic) uncertainties are displayed as error bars (boxes), while the global fully-correlated uncertainty is displayed as a box at unity.

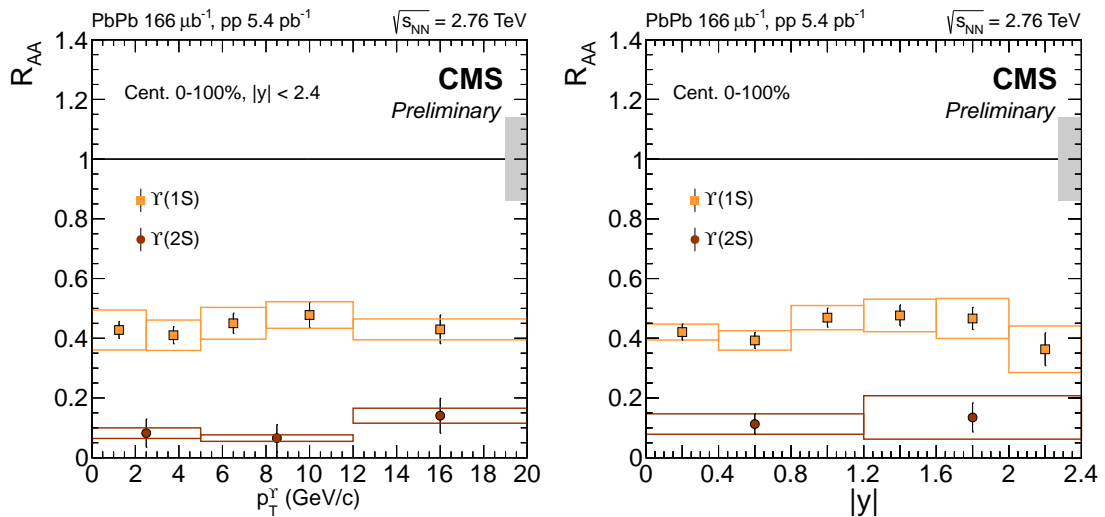


Figure 2. Nuclear modification factor of $\Upsilon(1S)$ and $\Upsilon(2S)$ in PbPb collisions as a function of transverse momentum (left) and rapidity (right). Statistical (systematic) uncertainties are displayed as error bars (boxes), while the global fully-correlated uncertainty is displayed as a box at unity.

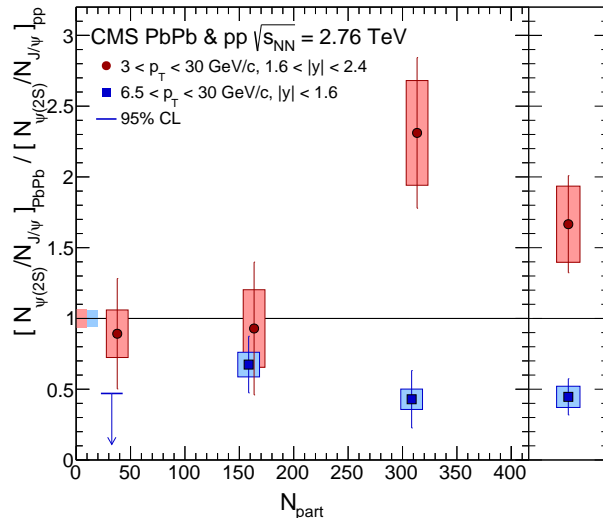


Figure 3. Measured yield double ratio as a function of centrality. The p_T and rapidity bins are $6.5 < p_T < 30$ GeV/c and $|y| < 1.6$ (left), and $3.0 < p_T < 30$ GeV/c and $1.6 < |y| < 2.4$ (right). The error bars and boxes stand for the PbPb statistical and systematic uncertainties, respectively. The shaded band is the uncertainty on the pp measurement, common to all double-ratio points.

For mid-rapidity, $|y| < 1.6$ the double ratio is always less than unity, meaning that $\psi(2S)$ are more suppressed than J/ψ . Within uncertainties, no centrality dependence is observed. However, going to the forward rapidity range, the data show an increase of the double ratio with centrality, though with large uncertainties. In the most central collisions the double ratio is about 1.7 which means that more $\psi(2S)$ are produced compared to J/ψ than in pp collisions, again with large uncertainties.

These results exhibit a clear $\psi(2S)$ suppression in the midrapidity and higher p_T region, while the pp uncertainty is too large to draw a firm conclusion in the forward rapidity lower p_T region.

3.3. Polarization of $\Upsilon(nS)$ in pp collisions

Polarization is a significant input to the non-relativistic QCD phenomenology of quarkonia production. In this model, the nonperturbative phenomenon of bound state formation involves the interaction with surrounding hadrons in the event. Therefore, the pre-resonant $Q\bar{Q}$ must neutralize its colour by absorbing or emitting soft gluons. It is natural to wonder whether the $Q\bar{Q}$ bound-state formation process could be different between pp and nucleus-nucleus collisions, or between “peripheral” and “central” pp collisions. So, polarization measurements can provide the cleanest indications on how the QCD medium surrounding the production of the $Q\bar{Q}$ pair affects its binding into the final-state quarkonium. The polarizations of the $\Upsilon(1S)$, $\Upsilon(2S)$, and $\Upsilon(3S)$ mesons produced in pp collisions at 7 TeV have been determined as a function of the charged particle multiplicity of the event, in two p_T ranges. [7]

To maximize the physical information and avoid interpretation ambiguities in comparisons with calculations or other experimental measurements [8], the three frame-dependent angular anisotropy parameters, $\vec{\lambda} = (\lambda_\vartheta, \lambda_\varphi, \lambda_{\vartheta\varphi})$, as well as the frame-invariant parameter [9] $\tilde{\lambda} = (\lambda_\vartheta + 3\lambda_\varphi)/(1 - \lambda_\varphi)$, are measured in three frames, with different directions of the quantization axis: the center-of-mass helicity (HX) frame, where the polar axis coincides with the direction

of the Υ momentum; the Collins–Soper (CS) frame, whose axis is the average of the two beam directions in the Υ rest frame; and the perpendicular helicity (PX) frame, orthogonal to the CS frame.

Figure 4 displays the corresponding results for the frame-invariant parameter $\tilde{\lambda}$. The results obtained in the CS, HX, and PX frames also showed good agreement. No significant changes of the polarizations are seen as a function of N_{ch} , for any of the three states.

3.4. J/ψ in pPb

The rapidity dependence of the J/ψ production can provide key information on the nPDFs and other CNM effects. The effect was quantified by investigating the forward-to-backward production ratio R_{FB} defined by

$$R_{\text{FB}}(p_{\text{T}}, y) = \frac{d^2\sigma(p_{\text{T}}, y > 0)/dp_{\text{T}}dy}{d^2\sigma(p_{\text{T}}, y < 0)/dp_{\text{T}}dy}, \quad (1)$$

where the $d^2\sigma/dp_{\text{T}}dy$ is the J/ψ production cross section decayed into muon pairs in a given p_{T} and y bin, and forward regions ($y > 0$) are defined by the proton-going direction.

Fig. 5 shows the p_{T} dependence of R_{FB} in three different rapidity ranges for prompt J/ψ . The data points are plotted at the bin-averaged values. The R_{FB} is closer to unity at high p_{T} , and decreases at low p_{T} . No strong rapidity dependence has been observed.

The R_{FB} of prompt J/ψ is further analyzed in terms of an event activity variable $E_{\text{T}}^{\text{HF}|\eta|>4}$, the transverse energy deposited in the forward hadronic calorimeter in $4 < |\eta| < 5.2$. The centers of the bin abscissae are given by their bin-averaged values, but slightly shifted for higher p_{T} points (left) or higher rapidity points (right), so that they do not overlap with each other. The clear decreasing tendency of the R_{FB} with increasing $E_{\text{T}}^{\text{HF}|\eta|>4}$ has been observed over the whole kinematic ranges, and it is more pronounced at low p_{T} in the forward rapidity region.

3.5. B^+ , B_s^0 , B^0 in pPb

The study of CNM effects is extended to heavy-quark production by performing the first measurement of exclusive B meson decays in pPb collisions. The R_{AA} and R_{FB} of B mesons are measured above transverse momentum of 10GeV/c.

The p_{T} -differential production cross sections of all three B mesons in the interval $|y_{\text{lab}}| < 2.4$ are measured [10], with data points placed at the center of each bin. They are compared to the pp cross sections obtained from fixed-order plus next-to-leading-logarithm (FONLL) calculations [11]. The FONLL predictions are scaled by $A(=208)$, the atomic mass of the Pb nucleus, to account for the number of binary NN collisions. The FONLL uncertainties, larger than the ones from data, represent the quadratic sum of several variations made to the calculation: of the factorization and renormalisation scales, of the c quark mass, and of the uncertainty associated with PDFs (providing the largest contribution) [11, 12, 13].

The theoretical uncertainties represented by the open blue boxes in Fig. 6 are computed by recalculating $R_{\text{pA}}^{\text{FONLL}}(p_{\text{T}})$ with the upper and lower values of the FONLL predictions. The nuclear modification factors of the three B mesons do not show evidence for modification of pPb data compared to the FONLL reference, in the considered p_{T} range within the quoted uncertainties. No significant differences are observed between the three B meson species.

The production cross section of B^+ is also studied as a function of its rapidity in the center-of-mass frame (y_{CM}). The y_{CM} -differential cross section of B^+ in the interval $10 < p_{\text{T}} < 60\text{GeV}/c$ is shown in Fig. 7 (left). In Fig. 7 (right), the rapidity dependence of the nuclear modification factor of B^+ is shown. No strong evidence of rapidity dependence of $R_{\text{pA}}^{\text{FONLL}}$ is observed within the uncertainties.

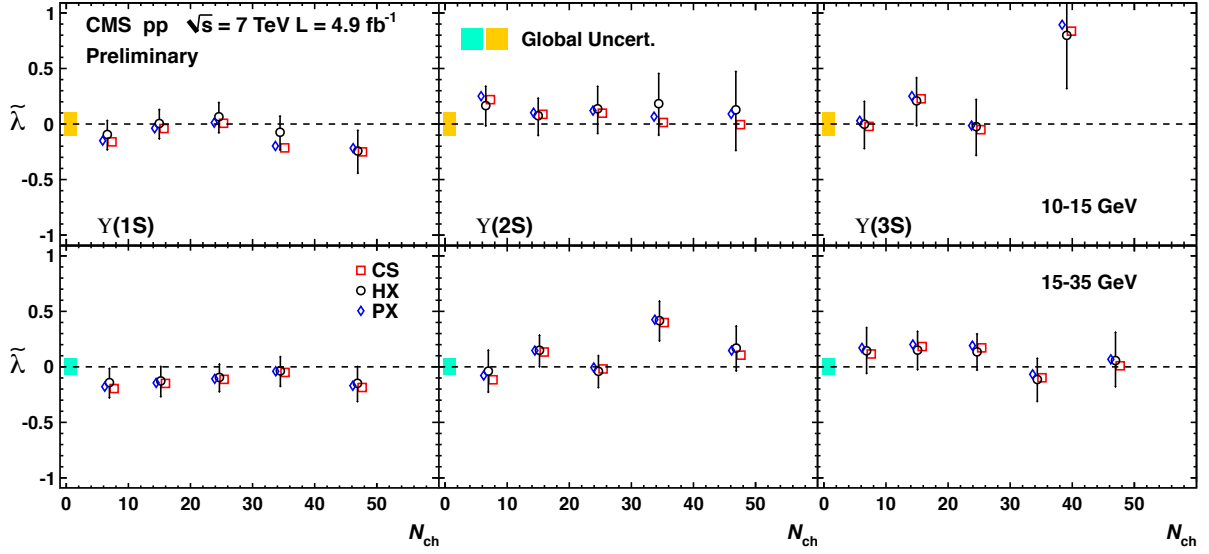


Figure 4. Values of $\tilde{\lambda}$ for the $\Upsilon(1S)$, $\Upsilon(2S)$, and $\Upsilon(3S)$ states (left to right), in the HX, CS, and PX frames. The vertical bars represent the 68.3% CL intervals of the total uncertainties, while the global uncertainties are represented by boxes at the zero horizontal line. The points have been slightly offset for easier viewing.

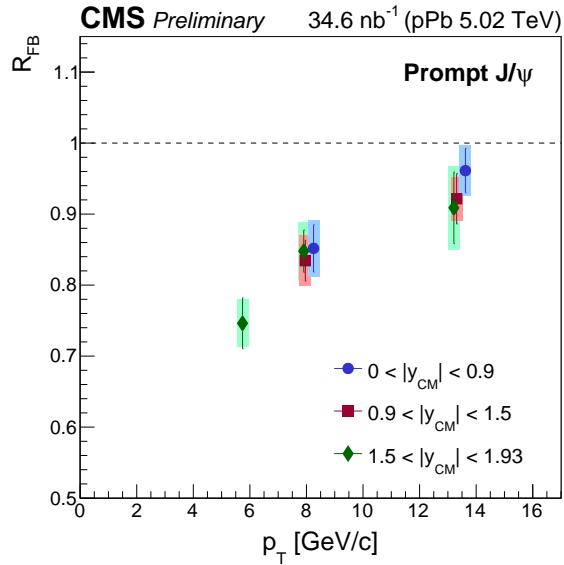


Figure 5. p_T dependence of R_{FB} for prompt J/ψ in three rapidity ranges. The error bars show the statistical uncertainties, and the shaded boxes represent the quadratic sum of systematic uncertainties.

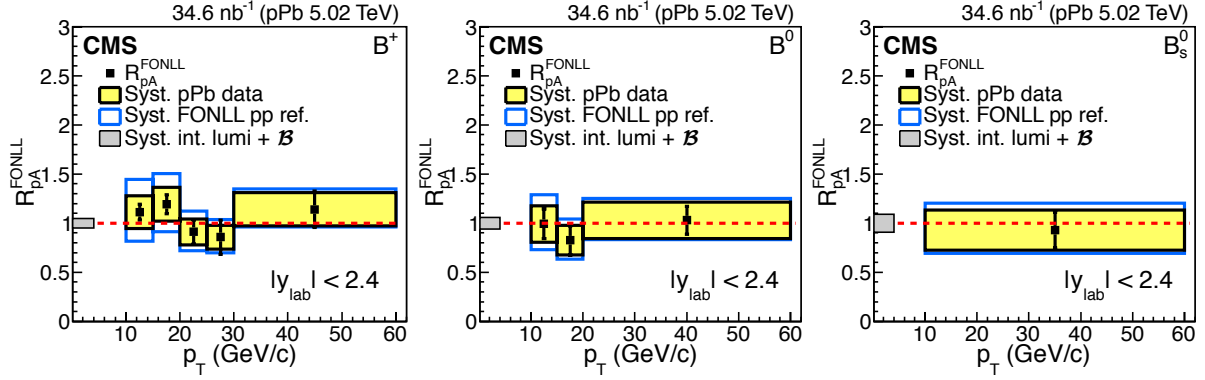


Figure 6. The nuclear modification factors $R_{pA}^{\text{FONLL}}(p_T)$ of B^+ (left), B^0 (center), B_s^0 (right) measured in pPb collisions at 5.02 TeV. The statistical and systematic uncertainties on the pPb data are shown as bars and yellow boxes around the data points, respectively.

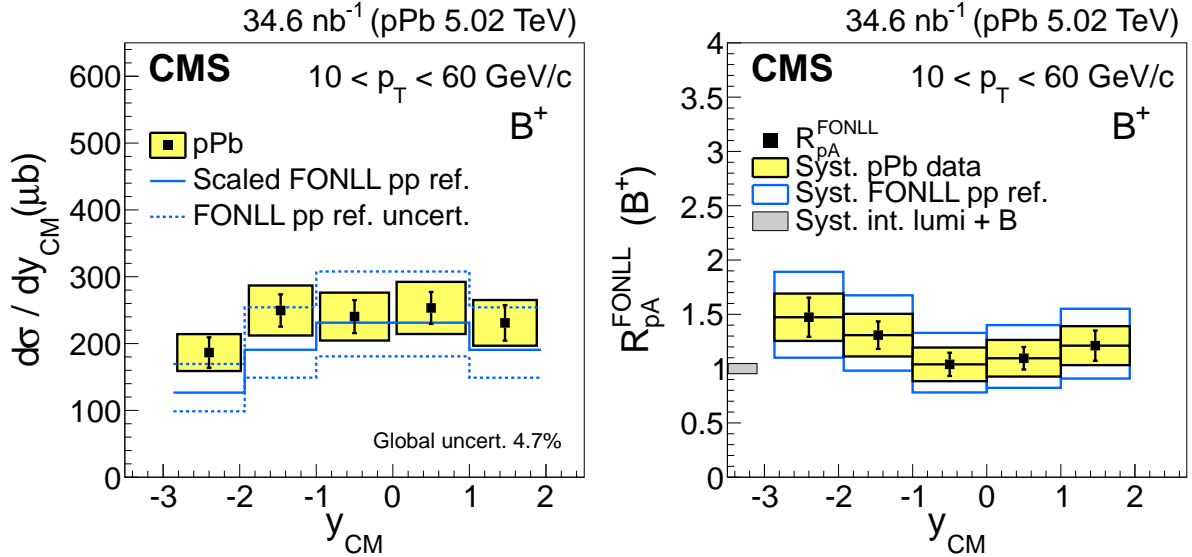


Figure 7. (left) The y_{CM} -differential production cross section of B^+ measured in pPb collisions at 5.02 TeV. Vertical bars (boxes) correspond to statistical (systematic) uncertainties. The listed global systematic uncertainty is not included in the data points. The result is compared to a FONLL calculation [12, 13, 11] represented by a continuous histogram. The dashed histograms represent the theoretical uncertainties for the FONLL reference. (right) The nuclear modification factor R_{pA}^{FONLL} of B^+ as a function of y_{CM} . The statistical and systematic uncertainties on the pPb data are shown as bars and yellow boxes around the data points, respectively. The systematic uncertainty from the FONLL reference is plotted separately as open blue boxes. The global systematic uncertainty is shown as a full grey box at unity, and is not included in the data points.

4. Summary

Recent results of quarkonia and B mesons from CMS heavy ion experiment were reviewed. $\Upsilon(1S)$, $\Upsilon(2S)$ and $\Upsilon(3S)$ meson yields have been measured in PbPb and pp collisions at the same energy per nucleon pair, $\sqrt{s_{NN}} = 2.76$ TeV. The $\Upsilon(1S)$ and $\Upsilon(2S)$ are suppressed by a factor of ≈ 2 and 10, respectively, while the unobserved $\Upsilon(3S)$ corresponds to a suppression by

a factor larger than 7, at 95% confidence level. Though a strong centrality dependence of the suppression is observed for the $\Upsilon(1S)$ and $\Upsilon(2S)$, no noticeable dependence is observed as a function of transverse momentum or rapidity.

The modification of the $\psi(2S)$ meson production and its ratio to J/ψ in PbPb was also discussed. At lower p_T , the data suggest an enhancement of the $\psi(2S)$ to J/ψ ratio, with respect to the corresponding pp measurement, that increases with PbPb collision centrality. Both the centrality dependence and the double ratio being larger than unity are opposite to the expected behavior in the sequential melting scenario.

The polarization of $\Upsilon(1S)$, $\Upsilon(2S)$ and $\Upsilon(3S)$ in pp collisions and their dependence on the particle multiplicity was investigated to observe the surrounding materials's effect to the angular states of quarkonia. There was not evidence of interference in high multiplicity pp collisions, however this study opens the way for analogous measurements in pPb and PbPb, which can provide the cleanest indications on how quark-antiquark bound-state formation is influenced by the surrounding medium, an essential input for the interpretation of quarkonium nuclear suppression patterns.

In the end, the measurement of prompt and non-prompt J/ψ and B mesons in pPb collisions at $\sqrt{s_{NN}} = 5.02$ TeV has been reported to discuss the cold nuclear matter effects. For J/ψ , the forward-to-backward production ratio R_{FB} is observed to be smaller than unity at low p_T and become consistent with unity for p_T above 10GeV/c. The R_{FB} and R_{AA} of B mesons were found to be consistent to unity in the overall measurement ranges, p_T above 10GeV/c, which is consistent to J/ψ result.

5. References

- [1] T. Matsui, H. Satz, J/ψ suppression by quark-gluon plasma formation, Phys. Lett. B 178 (1986) 416. doi:10.1016/0370-2693(86)91404-8.
- [2] A. Andronic, et al., Heavy-flavour and quarkonium production in the LHC era: from proton-proton to heavy-ion collisions, arXiv:1506.03981.
- [3] S. Chatrchyan, et al., The CMS experiment at the CERN LHC, JINST 3 (2008) S08004. doi:10.1088/1748-0221/3/08/S08004.
- [4] V. Khachatryan, et al., Measurements of Inclusive W and Z Cross Sections in pp Collisions at $\sqrt{s} = 7$ TeV, JHEP 1101 (2011) 080. arXiv:1012.2466, doi:10.1007/JHEP01(2011)080.
- [5] CMS Collaboration, Nuclear modification of Y states in PbPb, Tech. Rep. CMS-PAS-HIN-15-001, CERN, Geneva (2015).
URL <https://cds.cern.ch/record/2030083>
- [6] CMS Collaboration, Observation of sequential Upsilon suppression in PbPb collisions, Phys. Rev. Lett. 109 (2012) 222301. arXiv:1208.2826, doi:10.1103/PhysRevLett.109.222301.
- [7] CMS Collaboration, Measurement of the $Y(nS)$ polarizations in pp collisions as a function of charged particle multiplicity, Tech. Rep. CMS-PAS-HIN-15-003, CERN, Geneva (2015).
URL <http://cds.cern.ch/record/2030082>
- [8] P. Faccioli, C. Lourenço, J. Seixas, H. Wöhri, Towards the experimental clarification of quarkonium polarization, Eur. Phys. J. C 69 (2010) 657. arXiv:1006.2738, doi:10.1140/epjc/s10052-010-1420-5.
- [9] P. Faccioli, C. Lourenço, J. Seixas, New approach to quarkonium polarization studies, Phys. Rev. D 81 (2010) 111502(R). arXiv:1005.2855, doi:10.1103/PhysRevD.81.111502.
- [10] CMS Collaboration, Study of B meson production in pPb collisions at $\sqrt{s_{NN}} = 5.02$ TeV, arXiv:1508.06678.
- [11] M. Cacciari, S. Frixione, N. Houdeau, M. L. Mangano, P. Nason, G. Ridolfi, Theoretical predictions for charm and bottom production at the LHC, JHEP 10 (2012) 137. arXiv:1205.6344, doi:10.1007/JHEP10(2012)137.
- [12] M. Cacciari, M. Greco, P. Nason, The p_T spectrum in heavy-flavour hadroproduction, JHEP 05 (1998) 007. arXiv:hep-ph/9803400, doi:10.1088/1126-6708/1998/05/007.
- [13] M. Cacciari, P. Nason, Charm cross sections for the Tevatron Run II, JHEP 09 (2003) 006. arXiv:hep-ph/0306212, doi:10.1088/1126-6708/2003/09/006.